

Molecular Insights into Interactions between Ofloxacin and Ionic Micelles

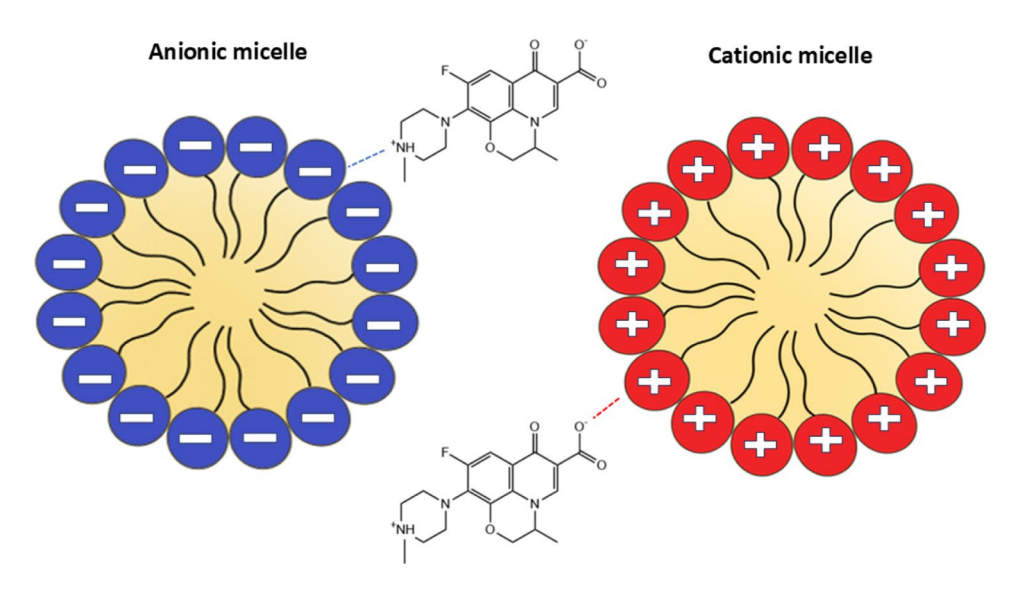
Saqib Rabbani¹ · Areesha Maryam¹ · Muhammad Sohail² · Athar Yaseen Khan¹

Received: 9 May 2025 / Accepted: 15 July 2025 © The Author(s), under exclusive licence to Springer Science+Business Media, LLC, part of Springer Nature 2025

Abstract

The growing antimicrobial resistance presents a challenge in developing new potent drugs, but this effort is hindered by a lack of information regarding how these new drugs would behave in biomembranes. Surfactants are considered mimetic models for biomembranes and can be used to study drug—membrane interactions. In this study, we used two well-known surfactants—cationic cetyltrimethylammonium bromide and anionic sodium dodecyl sulfate—as model membranes to investigate their interaction with the antimicrobial drug ofloxacin (OFL). These interactions were studied using volumetric and acoustic methods over the temperature range of 293.15–323.15 K to determine the apparent molar volume, isentropic compressibility, apparent molar compressibility, acoustic impedance, relative association, and intermolecular free length. Furthermore, UV–Vis spectroscopy and cyclic voltammetry were employed to evaluate the binding constants and free energies of the drug–surfactant systems. These results provide key molecular insights into the thermodynamics of OFL partitioning and its binding mechanisms with amphiphilic assemblies. Such mechanistic understanding is crucial for the rational design of antibiotic delivery systems, facilitating precise control over drug loading and release dynamics in surfactant-based formulations.

Graphical Abstract



 $\textbf{Keywords} \ \ Of loxacin \cdot Ionic \ surfactants \cdot Binding \ and \ partitioning \ parameters \cdot Volumetric \ studies \cdot Spectroscopy \cdot Cyclic \ voltammetry$

Extended author information available on the last page of the article

Published online: 22 July 2025



Introduction

Since the 1940s, antibiotics have played a vital role in the treatment of infectious diseases. For several decades, pharmaceutical companies made steady progress in developing new antimicrobial agents. However, this progress slowed significantly after the 1980s (Christaki et al. 2020). The resulting decline in antibiotic innovation has contributed substantially to the rise of antibiotic resistance, a phenomenon in which bacteria acquire the ability to survive exposure to drugs intended to eliminate them. The widespread presence of antibiotics in the environment further exacerbates this problem, accelerating the development of resistance. Addressing this growing threat has become a critical global health priority, underscoring the urgent need for new and effective therapeutic strategies (Duval et al. 2019).

Beyond antibiotic resistance, one of the persistent challenges in medical treatment is the inconsistent or inefficient delivery of drugs to their target sites. Traditional drug delivery methods often fail to effectively traverse biological barriers, leading to suboptimal therapeutic outcomes. These conventional systems typically lack the capacity for precise targeting and sustained drug release. To overcome these limitations, researchers are developing advanced delivery platforms capable of accurately controlling dosage and directing drugs to specific locations, thereby enhancing treatment efficacy (Liu et al. 2016).

A thorough understanding of how medications interact with biological membranes is essential for refining therapeutic strategies. To investigate these interactions, researchers have employed various model systems, including bicelles, micelles, and lipid monolayers and bilayers (Sohail et al. 2020). Among these, micelles have attracted significant attention due to their potential as efficient drug carriers. This effectiveness arises from the unique characteristics of surfactants, which naturally form nanoscale structures (Chen and Panagiotopoulos 2019). Surfactants consist of hydrophilic head groups and hydrophobic tails, enabling them to spontaneously assemble into micelles once their concentration exceeds a specific threshold known as the critical micelle concentration (CMC) (Kumar and Rub 2018a, 2018b). This self-assembly behavior makes micelles valuable not only in pharmaceutical applications but also in fields such as nanotechnology, food science, and personal care (Chen and Panagiotopoulos 2019).

Ionic surfactants, in particular, can form micelles, vesicles, and bilayers in aqueous solutions, mimicking the structure and behavior of natural biological membranes (Castillo-Sánchez et al. 2021). These model systems provide critical insights into membrane properties such as

permeability, fluidity, and lipid-protein interactions under controlled conditions. The charged nature of ionic surfactants also enables researchers to explore electrostatic interactions relevant to cellular membranes. Such systems are instrumental in advancing our understanding of membrane-associated processes and hold significant promise for improving drug delivery technologies and designing synthetic cells (Alalwani et al. 2023). Continued research in this field has the potential to yield more effective strategies for combating antibiotic resistance and enhancing therapeutic outcomes.

Ofloxacin (OFL), a broad-spectrum fluoroquinolone antibiotic, is widely prescribed for the treatment of bacterial infections, including those caused by Mycobacterium (e.g., leprosy) and *Chlamydia* species (Eid et al. 2019; Pathania et al. 2016). It exhibits strong efficacy against both Grampositive and Gram-negative bacteria (Suresh et al. 2020). While previous studies have explored the interactions of OFL with ionic and nonionic surfactants—primarily focusing on micellization behavior, complexation for drug delivery, or environmental removal of antibiotics—these investigations have not addressed the fundamental mechanism of OFL transport across membrane-mimetic systems (Ghosh et al. 2019; Ahmed et al. 2024a, b). In this study, we aim to elucidate the diffusion behavior of OFL through surfactant-based model membranes, providing a mechanistic understanding of its interaction dynamics. Such knowledge is particularly valuable for guiding the rational design of next-generation antibiotic drugs with improved membrane permeability and therapeutic efficiency.

Volumetric and acoustic techniques have proven effective for analyzing solute–solvent interactions in drug–surfactant systems (Sharma and Chauhan 2014). These methods facilitate a detailed investigation of molecular packing, solvation behavior, and intermolecular forces. They also provide thermodynamic insights into hydration patterns, aggregate stability, and the spatial positioning of drug molecules within micelles, whether embedded in the hydrophobic core or located in the outer region.

In this context, key physicochemical properties—including apparent molar volume (ϕ_v), apparent molar compressibility (ϕ_k), isentropic compressibility (K_s), acoustic impedance (Z), relative association (RA), and intermolecular free length (L_f)—were measured for OFL–CTAB and OFL-SDS systems over the temperature range of 293.15 to 323.15 K. Complementary studies on binding constants, partition coefficients, and standard free energy changes further elucidate the mechanisms governing these drug–surfactant interactions (Mahajan et al. 2012). Collectively, these analytical approaches provide deeper insight into drug behavior in complex systems, facilitating the development of advanced delivery platforms that enable controlled release and improved bioavailability. This comprehensive strategy lays



Fig. 1 Chemical structures of a OFL, b CTAB, and c SDS

a solid foundation for enhancing the therapeutic efficacy of antibiotics in pharmaceutical applications (Fig. 1).

Materials and Methods

Materials

Cetyltrimethylammonium bromide (CTAB, purity \geq 99%) and sodium dodecyl sulfate (SDS, purity \geq 99%) were purchased from Sigma-Aldrich Co. (St. Louis, MO, USA). OFL (purity \geq 99%) was obtained from Schazoo Zaka (Pvt.) Ltd., Lahore, Pakistan. All reagents were used without further purification.

A 0.1 M phosphate buffer solution (PBS) at pH 7.4 was prepared using disodium hydrogen phosphate (Na₂HPO₄, \geq 98% purity), and the pH was adjusted using concentrated sodium dihydrogen phosphate (Na₂HPO₄, \geq 98% purity). All solutions were prepared with distilled water.

Methods

Volumetric, acoustic, and spectroscopic measurements were conducted at a controlled room temperature of 25.0 ± 0.1 °C to simulate physiological conditions. A primary solution of OFL (1 mM) was initially prepared in distilled water, which was subsequently used to formulate CTAB (6 mM) and SDS (21 mM) mixtures. For UV–Visible spectroscopic analysis, the OFL solution was further diluted to a final concentration of 2.20×10^{-5} mol dm⁻³ to ensure compliance with the Beer–Lambert law. Spectral data were recorded using

a UV–Visible spectrophotometer, with distilled water serving as the reference baseline. For post-micellar phase measurements, OFL itself was used as the reference standard. A series of CTAB (0.3 to 4 mM) and SDS (2.5 to 15 mM) solutions were prepared while maintaining a constant OFL concentration throughout the experiments. The standard uncertainties in pressure (P), temperature (T), molality (m), density (d), and ultrasonic velocity (u) were \pm 0.1 kPa, \pm 0.0 1 K, \pm 0.20 × 10⁻³ mol kg⁻¹, \pm 0.16 kg m⁻³ and \pm 0.51 m s⁻¹, respectively.

Density and Sound Velocity Measurements

Density and sound velocity measurements for the OFL-CTAB and OFL-SDS systems were performed using an Anton Paar DSA 5000 density and sound velocity meter. Measurements were conducted over a temperature range of 293.15 to 323.15 K, in 5 K increments.

Spectroscopic Studies

UV–Visible absorption studies of the OFL-CTAB and OFL-SDS systems were conducted at 298.15 K using a Shimadzu UV-1800 spectrophotometer equipped with a quartz cuvette of 0.01 m path length.

Electrochemical Studies

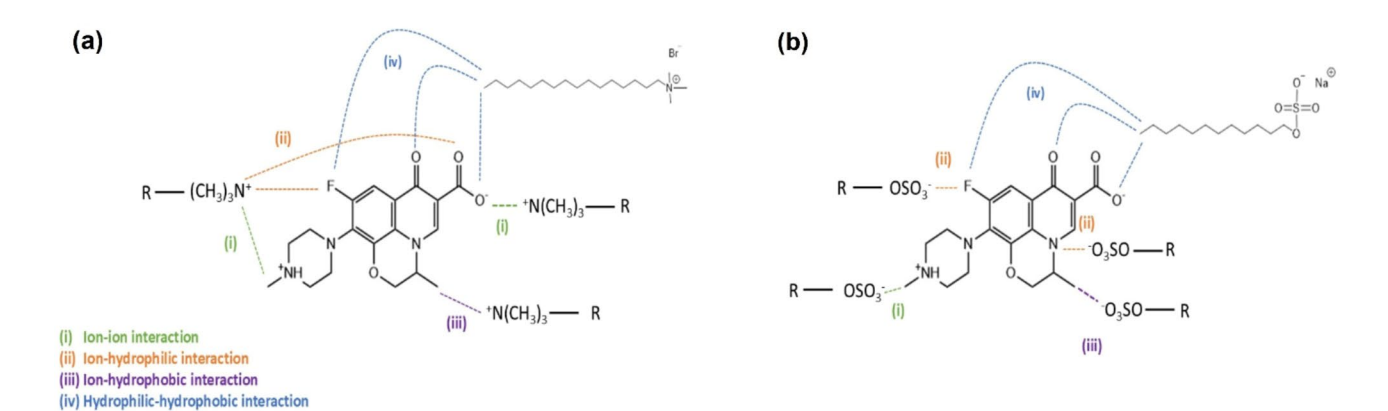
For electrochemical investigations, cyclic voltammetry measurements were performed using a computer-aided eDAQ potentiostat system (Model ED401). A conventional three-electrode setup was employed, consisting of a 1 mm diameter glassy carbon electrode as the working electrode, a platinum wire as the auxiliary electrode, and an Ag/AgCl electrode as the reference electrode. Cyclic voltammograms of OFL (1 mM) in PBS containing CTAB (6 mM) and SDS (21 mM) surfactants were recorded at a scan rate of 100 mV s⁻¹. Before each measurement, the working electrode was polished using an alumina powder slurry. All measurements were conducted at 298.15 K.

Results and Discussion

Volumetric and Compressibility Studies

The experimental density and sound velocity values of OFL-CTAB and OFL-SDS as a function of surfactant concentration are provided in Tables S1–S4 of the supplementary information. The Eq. (1) was employed to calculate (Sohail et al. 2020) apparent molar volume (ϕ_{ν}) data of CTAB and SDS, and the data for both systems are given in Tables S5 and S6:





Scheme 1 Schematic representation of the possible types of interactions occurring in the (a) OFL-CTAB and (b) OFL-SDS systems

$$\phi_{v} = \frac{M}{d} + \frac{\left[d_{o} - d\right]}{mdd_{o}} \tag{1}$$

Here, M denotes the molar mass of the surfactant (g mol⁻¹), d is the density of the solution, d_0 represents the density of the pure solvent, and m (mol kg⁻¹) corresponds to the solution's molality.

The *m* of the solution was determined using molar concentration values by employing the following relation: $m = 1/[\frac{d}{c} - \frac{M}{1000}]$, where *C* (mol dm⁻³) represent the molar concentration of the surfactant, respectively.

Understanding the molecular interactions between OFL and ionic surfactants such as CTAB and SDS is essential for elucidating its solvation dynamics and microenvironment within micellar systems. The following types of interactions are expected in these systems and are illustrated in Scheme 1 below: (1) ion-ion interactions between the protonated NH⁺ moiety of OFL and the counterions of surfactants, such as Br in CTAB or OSO₃ groups of SDS. In contrast, the carboxylate group (-COO⁻) of OFL can interact electrostatically with the positively charged -N⁺(CH₃)₃ headgroup of CTAB and Na⁺ of SDS, but electrostatic repulsion would occur with the anionic sulfate group (-OSO₃⁻) of SDS; (ii) ion-hydrophilic interactions between the ionic head groups of the surfactants and the hydrophilic functional groups of OFL, including fluorine (-F), nitrogen (-N-), oxygen (-O-), and carbonyl (-C=O) groups; (iii) ion-hydrophobic interactions between the ionic head groups of the surfactants and hydrophobic regions of OFL (such as with π -electrons of aromatic part and alkyl moieties). Similar forces also exist between the hydrophobic alkyl chains of surfactants and ionic parts of the OFL; (iv) hydrophilic-hydrophobic interactions between hydrophilic regions of OFL and the alkyl chains of surfactants; (v) hydrophobic-hydrophobic interactions among the alkyl chains of surfactants with the nonpolar sites of OFL through van der Waals forces; (vi) hydrogen bonding among surfactants, OFL, and water molecules.

Overall, the volumetric and compressibility analyses offer meaningful insight into the molecular interactions that influence OFL's behavior within CTAB and SDS micellar systems. The variations observed in apparent molar volume (ϕ_v) further reflect the strength and character of solute–solvent and solute-surfactant interactions present in these environments.

The plot of ϕ_v with respect to m of CTAB and SDS in OFL is given in Fig. 2a and b, respectively. ϕ_{v} values are negative and increases towards less negative values with increasing both temperature and surfactant m, reaching at a plateau at higher concentrations. This can be explained by the well-known cosphere overlap model given by Frank and Evans (1945) and further modified by Gurney (Gurney 1953). When hydrated ions in solution approach each other, their hydration shells may overlap, causing some structured water molecules to be released. This overlap can either increase entropy and be energetically favourable or disrupt strong ion-water interactions and be unfavorable. In 1953, R.W. Gurney expanded on this idea, explaining how varying degrees of overlap lead to either solvent-separated or contact ion pairs. For the amphiphilic molecules like OFL, the cospheres of its hydrophilic and hydrophobic regions exhibit distinct characteristics (Friedman and Krishnan 1973). His model also shows that hydrophobic group interations cause a negative volume change, while overlap of polar or ionic groups leads to a positive volume change (Yan et al. 2013).

For both OFL-CTAB and OFL-SDS systems (Fig. 2), the initial negative values for ϕ_v values at lower surfactant concentrations is primarily attributed to type (v) interactions between the nonpolar sites of OFL and the alkyl chains of both CTAB and SDS surfactant molecules. As the surfactant concentration increases, hydrophilic interactions (types (i), and (ii)) between drug and surfactant become more prominent, resulting increase in ϕ_v values. Eventually, at molal



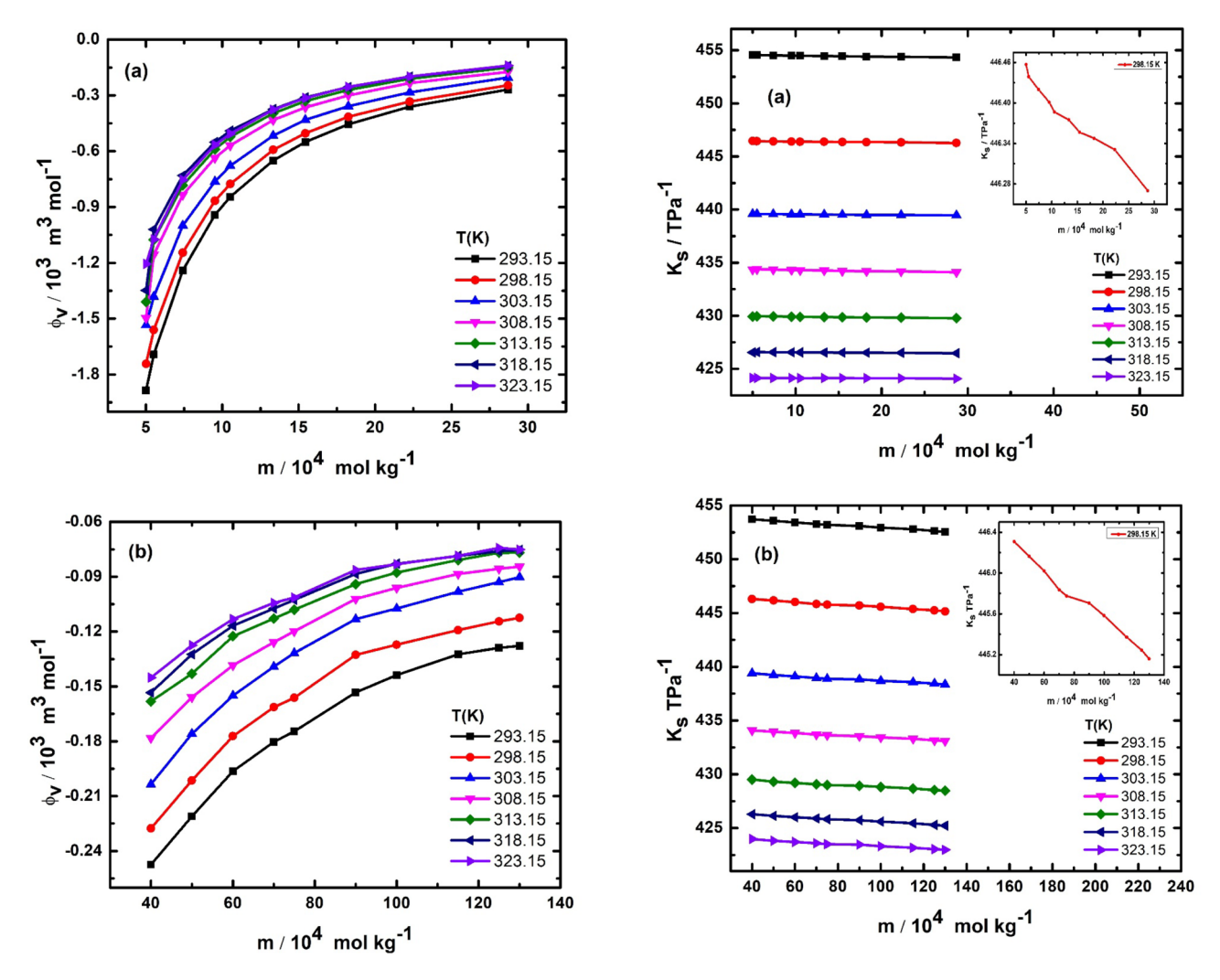


Fig. 2 Plot of ϕ_v against m of a CTAB in OFL (1 mM) and b SDS in OFL (1 mM) at various T

Fig. 3 The plot of K_s with respect to m of **a** CTAB in OFL (1 mM), **b** SDS in OFL (1 mM) at various T. Insets plot of K_s with respect to m of CTAB in OFL (1 mM), and SDS in OFL (1 mM) at 298.15 K

concentrations m \geq 14 for CTAB and m \geq 10 for SDS, ϕ_{ν} values become almost independent of surfactant concentration. This shows the point of micellization, wherein the surfactant molecules self-assemble into micelles, encapsulating OFL within their micellar structure and stabilizing the system. Similarly, by an increase in temperature, ϕ_{ν} values are also increasing, confirming the strengthening of types (i), and (ii) interaction between OFL and with both CTAB and SDS molecules.

The Tables S7 & S8 of supplementary information show Isentropic compressibility (K_s) data for OFL-CTAB and OFL-SDS systems computed using the given Eqs. (2) and (3). (Bhardwaj et al. 2014):

$$K_o = \frac{1}{d_o u_o^2} \tag{2}$$

$$K_s = \frac{1}{du^2} \tag{3}$$

where K_0 and K_s represent the isentropic compressibility of the pure solvent and solution, respectively. The parameters d_0 and d denote the densities of the solvent and solution, while u_0 and u correspond to the sound velocities of the solvent and solution.

 K_s data provide valuable understanding of the structural changes resulting from interactions of OFL with CTAB and SDS in solution (Fig. 3). In micellar systems, isentropic compressibility (K_s) is solely governed by two factors (1) Interactions between surfactant head groups, which influence micellar packing and electrostatic repulsion or attraction, and (2) compressibility of the hydrocarbon core, indicating the micellar interior's structural flexibility and its response to external perturbations. Additionally, the



hydrophilic nature and counter-ion binding of the surfactant head groups play a significant role in dictating the compressible nature of the solutions (Chauhan et al. 2012a).

As shown in the insets of Fig. 3a and b, a decline in K_s values with the increasing m of CTAB and SDS, suggesting the decrease in compressibility with m, indicating closer molecular packing and enhanced solute-solvent interactions. The interaction of the surfactant head groups and the compact arrangement of the hydrocarbon tails, coupled with strong associations of OFL with both CTAB and SDS, significantly restricts the movement of surrounding solvent molecules, resulting in the formation of a more rigid micellar environment (Chauhan et al. 2012b). A significant decline in K_s values with increasing temperature further supports this interpretation. The observed result indicates that thermal energy disrupts the structured water molecules present in the vicinity of the ionic surfactant monomers. As these hydrogen-bonded water molecules break apart, solute-solvent interactions become more evident, ultimately increasing the solubilization and interaction of OFL within the micellar environment. This trend aligns with volumetric observations, establishing the development of highly organized micellar structures at elevated surfactant concentrations.

The apparent molar compressibility (ϕ_k) values for CTAB and SDS, provided in Tables S9 and S10 of the supplementary information, were determined using Eq. (4). (Lomesh et al. 2019):

$$\phi_k = \phi_v K_s + \frac{\left[K_s - K_o\right]}{md_o} \tag{4}$$

where ϕ_k represents the apparent molar compressibility.

Figure 4 shows the change of ϕ_k with increasing m of CTAB and SDS. The observed trend indicates that ϕ_k values shift from highly negative towards less negative as surfactant concentration increases. This suggests a progressive loss of hydrophobic hydration due to the micellization of surfactants. As surfactants self-assemble into micelles, water molecules that were previously structured around the hydrophobic regions are expelled into the bulk phase, resulting in a more compressible micellar interior. The behavior of ϕ_k further confirms the trends observed in K_s , reestablishing the idea that OFL-CTAB and OFL-SDS interactions and micellar structuring contribute significantly to the compressibility behavior of the system. The nearly unvarying compressibility values across different concentrations mean that once micellization occurs, the system achieves a stable, well-organized structure with little further changes in molecular packing. In both OFL-CTAB and OFL-SDS systems, increasing the temperature results in higher ϕ_k values. The high temperature weakens ion-dipole attractions, promoting the release of water molecules previously bound to the ionic head groups of SDS and OFL. As these water molecules are

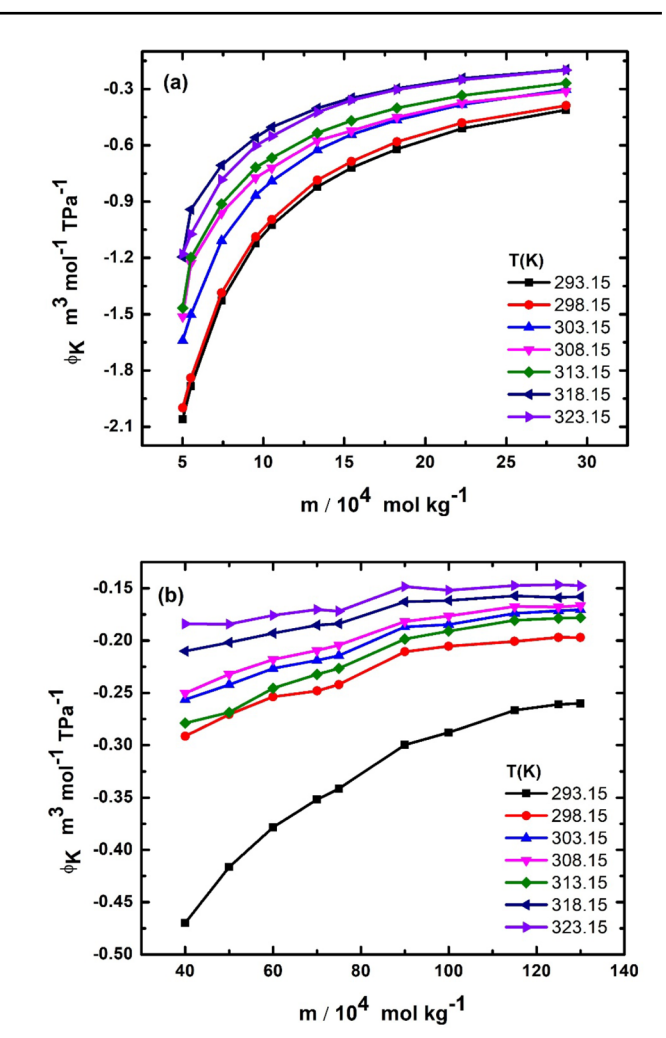


Fig. 4 The plot of ϕ_k against m of **a** CTAB in OFL (1 mM) and **b** SDS in OFL (1 mM) at various T

displaced into the bulk phase, the solution structure becomes less ordered, leading to enhanced molecular mobility. This shift contributes to an overall increase in the compressibility of the medium.

The acoustic impedance (*Z*) of the OFL-surfactant systems was computed using the following Eq. (5) (Santosh et al. 2009):

$$Z = u \times d \tag{5}$$

The relative association (*RA*), which provides insights into molecular association strength, was determined using the following relation (Eq. 6) (Rabbani et al. 2025):

$$RA = \left(\frac{d}{d_{\circ}}\right) \left(\frac{u_{\circ}}{u}\right)^{1/3} \tag{6}$$

The intermolecular free length (L_f) between two molecules, estimated using Jacobson's equation (Nadeem et al. 2024), is given by Eq. (7):



$$L_f = \frac{K}{ud^{\frac{1}{2}}} \tag{7}$$

where, $K = [(93.875 + 0.375) T \times 10^{-8}]$ (Nadeem et al. 2024). The computed data of Z, RA, and L_f for OFL-surfactant systems are given in Tables S11–13, further explaining the nature of molecular interactions within the system. Figure 5a and b shows the change of Z with increasing m of CTAB and SDS. Notably, an increase in Z values (Table S11) with rising surfactant concentration suggests enhanced electrostatic interactions between OFL and the respective ionic surfactants (Naseem and Iftikhar 2017). This trend implies that the incorporation of OFL into the micellar environment leads to a denser molecular packing, reducing the compressibility of the solution and strengthening intermolecular interactions.

The RA parameter explains key insights into molecular interactions within a solution. Its value depends on how solute molecules change the solvent's structure and their solvation behavior (Naseem 2020). In Table S12, the RA measurements for OFL-surfactant systems are detailed, and the plot of change in RA with increasing m of CTAB and SDS is shown in Fig. 5c and d. In the case of the OFL-CTAB system, there is a noticeable decrease in RA values as the concentration of CTAB increases. This suggests that the solvation of ions in the OFL-CTAB system is diminishing, likely due to the micellization process. As CTAB molecules aggregate into micelles, the solvating effect on the ionic species of OFL decreases, leading to a reduction in the relative association. On the other hand, for the SDS-OFL system, the RA values increase with rising molality of SDS, indicating an enhanced solvation of ions in this system. The increase in RA suggests that as more SDS molecules are added, the ionic head groups of SDS interact more effectively with the ionic groups of OFL, increasing the solvation of both components. This behavior highlights the role of SDS in forming a more solvation-rich environment around the solute, stabilizing the system through stronger solute-solvent interactions.

 L_f represents the gap between nearby molecules in a solution. This distance is determined by a combination of interand intra-molecular distances, which govern the spatial organization and density of the solution's molecular structure. Such interactions are crucial in bridging the connection between free length and adiabatic compressibility (Asghar Jamal et al. 2020). Figure 5e and f shows the change of L_f with increasing m of CTAB and SDS. The data (Table S13) reveal a consistent decrease in L_f values as the m of CTAB and SDS increases. This behavior indicates the robust solute–solvent interactions between OFL and the surfactants. At higher concentrations of CTAB or SDS, these interactions become more pronounced, effectively compressing the intermolecular spacing. The observed decline in L_f further indicates that OFL acts as a structure-promoting agent in

these surfactant systems (Naseem and Iftikhar 2017). The reduced intermolecular free length means that the molecules are being drawn closer together due to stronger solute—solvent interactions and the structuring effect induced by the surfactants. This behavior further manifests the formation of well-organized micellar structures and reflects the ability of the surfactant to organize the solute molecules more tightly in the solution.

Spectroscopic Studies

The absorption spectra of the OFL-CTAB and OFL-SDS systems under biological conditions (pH 7.4) are shown in Fig. 6a and b, respectively. The insets of Fig. 6a and b show the changes in absorbance and the corresponding shifts in maximum absorption wavelength (λ_{max}) with respect to the concentrations of CTAB and SDS, respectively. These variations reflect the concentration-dependent changes in the electronic environment of the OFL molecule, which are influenced by interactions with the surfactant head groups. As the concentration of either surfactant increases, significant changes in the absorbance spectrum and λ_{max} can indicate solute—solvent and surfactant-solute interactions, suggesting possible changes in the molecular conformation or aggregation state of OFL.

A significant change in absorbance, mixed with a shift in λ_{max} , occurs at 8.95 mM [CTAB] and 2.22 mM [SDS], suggesting the incorporation of OFL into the micellar structures of these surfactants at these concentrations. These spectral changes indicate the point at which OFL molecules are encapsulated within CTAB and SDS micelles, marking the beginning of robust surfactant-solute interactions.

Additionally, the visible absorption spectrum of OFL shows a concentration-dependent shift in λ_{max} from 291 to 287 nm in the presence of both surfactants. This shift suggests that OFL primarily interacts with the headgroups of CTAB and SDS micelles, thereby altering its electronic environment. The observed blue shift in λ_{max} also points to a decrease in the dielectric constant of the surrounding medium, a hallmark of micelle formation. These changes demonstrate that interactions with surfactant micelles substantially modify the local solvent environment around the OFL molecule, hence affecting its spectroscopic properties. This behavior highlights the critical role of surfactant-mediated solubilization in shaping the molecular microenvironment of OFL at physiological pH.

Figure 7a and b present the differential absorbance spectra of OFL in CTAB and SDS solutions, respectively, at 298.15 K. The systematic enhancement in ΔA values with increasing surfactant concentration shows gradual micellar incorporation of OFL molecules. This concentration-dependent absorbance rise confirms greater OFL entrapment within the micellar assemblies at higher



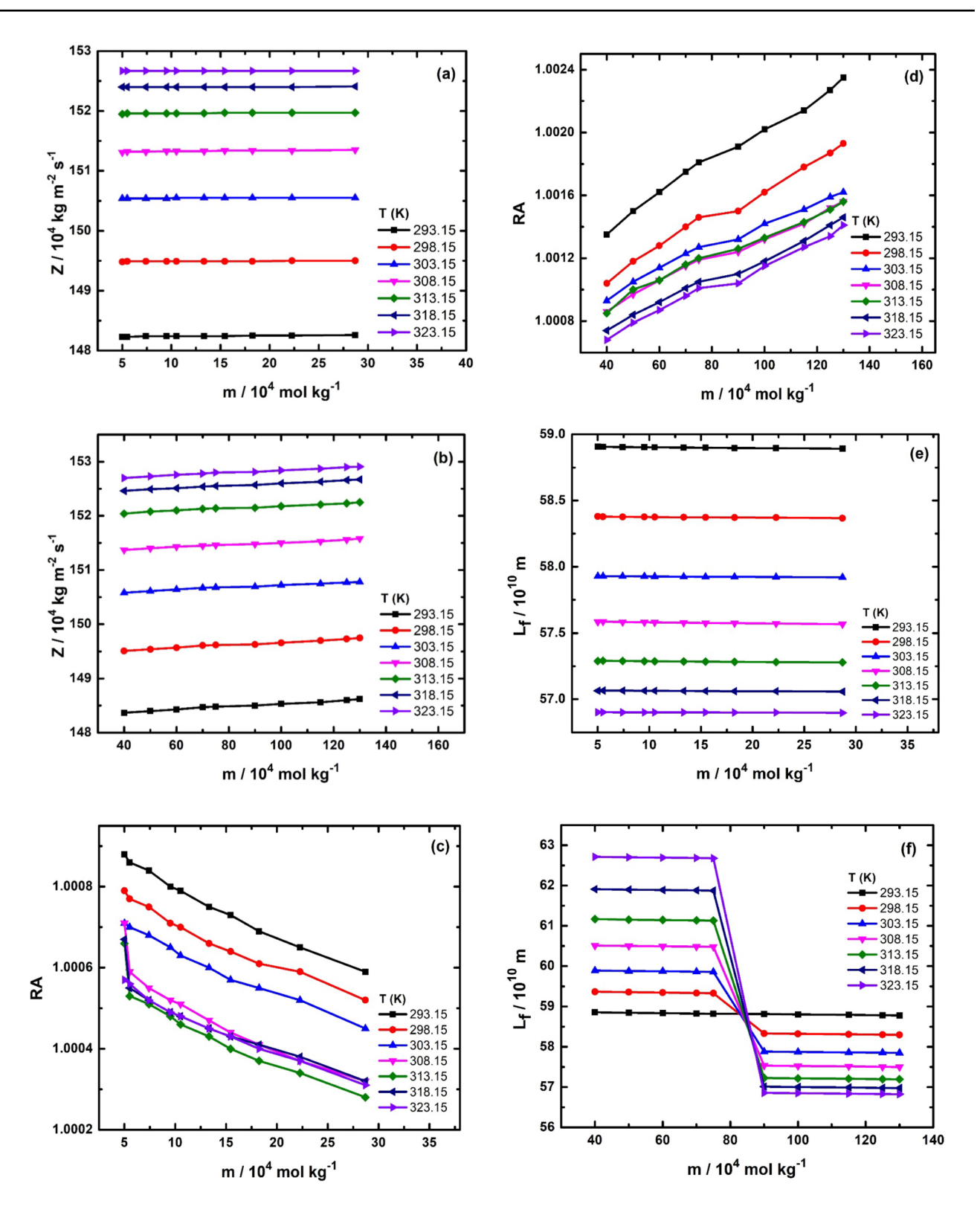


Fig. 5 Plots of a Z vs. m for CTAB in OFL (1 mM), b Z vs. m for SDS in OFL (1 mM), c RA vs. m for CTAB in OFL (1 mM), d RA vs. m for SDS in OFL (1 mM), e L_f vs. m for CTAB in OFL (1 mM), and f L_f vs. m for SDS in OFL (1 mM) at various T



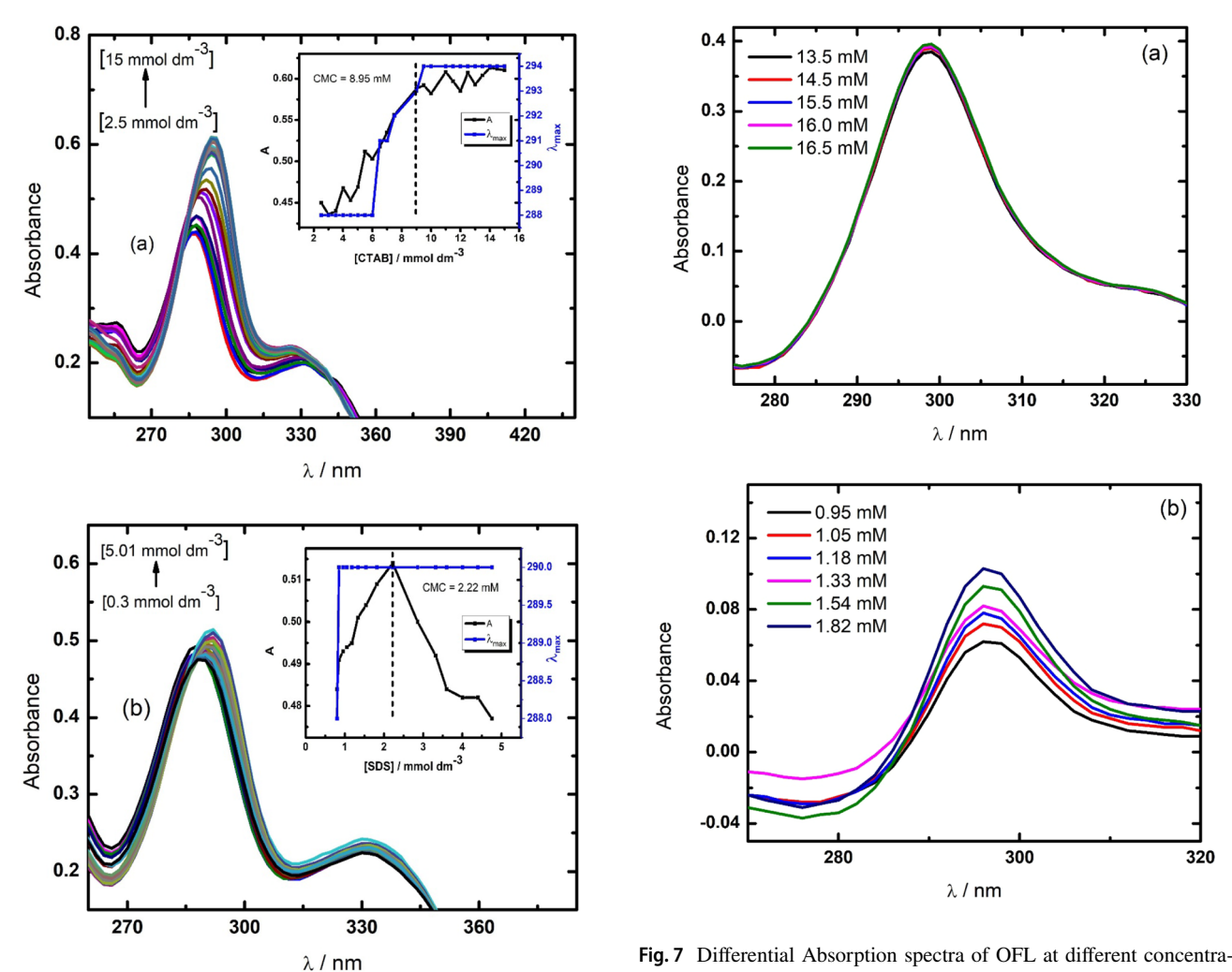


Fig. 6 Absorption spectra of OFL with a CTAB and (b) SDS. Insets: variation in absorbance and λ_{max} versus concentration of (a) CTAB and b SDS (at 298.15 K)

tions of a CTAB and b SDS (at 298.15 K)

 $\frac{1}{\Delta A} = \frac{1}{K_c \Delta A_m (C_a + C_m^{mo})} + \frac{1}{\Delta A_m}$

surfactant levels. The absence of substantial absorption band shifts suggests preservation of OFL's electronic transitions, consistent with molecular localization in both the hydrophobic micellar core and hydrophilic interfacial regions. This dual partitioning behavior sits well with the amphiphilic character of both OFL and the surfactant molecules (Faizan et al. 2015).

The partition coefficient (K_c) was calculated using the following parameters: C_a (drug concentration) and C_s^{mo} (effective micellar surfactant concentration), where $C_s^{mo} = C_s - \text{CMC}^0$ (with CMC⁰ being the surfactant's critical micelle concentration). The differential absorbance at infinite surfactant concentration is denoted as ΔA_{∞} . The K_c values were calculated from the slope-to-intercept ratio of the linear plot of $1/\Delta A$ versus $1/(C_a + C_s^{mo})$, as illustrated in Supplementary Information Fig. 7S(a) and 1S(b).

The partition coefficient (K_c) serves as a crucial thermodynamic indicator, calculating the degree of OFL solubilization within micellar systems. This parameter precisely characterizes the equilibrium distribution of OFL between micellar and aqueous phases, offering valuable insights into drug-membrane interactions and micellar encapsulation efficiency. To calculate this partitioning, the Kawamura model (Eq. 9) was employed (Kawamura et al. 1989), which allows for the quantification of the partition coefficient based on the observed changes in the absorbance spectra.

The partition constant (K_x) is calculated using Eq. (10):

$$K_x = K_c \times n_w \tag{10}$$

where n_w represents the number of moles of H_2O per dm³ of pure water (55.55 mol/dm³). The values of K_x and the free energy of partitioning (ΔG_p) are provided in Table 1. The large value of K_x (374.98 × 10³) indicates that OFL molecules are transferring from the aqueous medium



(9)

Table 1 Partition coefficient (K_x) , binding constant (K_b) , and Gibbs free energy of OFL-surfactant systems determined by UV–Visible spectroscopy and cyclic voltammetry

Surfactant system	em Spectroscopic results				Voltammetric results	
	$K_x \times 10^3$	$\Delta G_p (\mathrm{KJ} \; \mathrm{mol}^{-1})$	$K_b (\mathrm{M}^{-1}) \times 10^3$	$\Delta G_b (\mathrm{KJ} \; \mathrm{mol}^{-1})$	$\overline{K_b (\mathrm{M}^{-1}) \times 10^3}$	$\Delta G_b (\mathrm{KJ} \mathrm{mol}^{-1})$
OFL-CTAB	150.04 ± 0.35	-29.54 ± 0.45	0.083 ± 0.35	-10.95 ± 0.44	1.24 ± 0.08	-17.65 ± 0.11
OFL-SDS	374.98 ± 0.09	-31.81 ± 0.10	7.5 ± 0.09	-22.11 ± 0.10	6.08 ± 0.13	-21.59 ± 0.12

into the micellar environment, confirming that micellization is a favourable process for the solubilization of OFL. Correspondingly, the negative free energy of partitioning $(\Delta G_p = -31.81 \text{ kJ mol}^{-1})$ confirms that this partitioning process is also spontaneous. The higher K_x values observed for the OFL-SDS system indicate a stronger electrostatic interaction between the SDS surface and the negatively charged carboxylate group of OFL, which further facilitates the transfer of OFL into the micellar core.

The binding constant (K_b) , which indicates the strength of OFL-surfactant interactions, was derived from differential absorbance measurements using the Benesi-Hildebrand Eq. (11) (Benesi and Hildebrand 1949). This approach provides quantitative characterization of the binding affinity between OFL and the micellar assemblies, complementing the partition coefficient data.

$$\frac{dC_a}{\Delta A} = \frac{1}{(\Delta \varepsilon K_b C_s^{mo})} + \frac{1}{\Delta \varepsilon} \tag{11}$$

In this equation, the difference in absorption coefficients is represented as $\Delta \varepsilon$. The binding constant (K_b) was calculated using the intercept and slope values from the $dC_a/\Delta A$ vs. $1/C_s^{mo}$ plot, which is presented in Fig. 1S(a) and 2S(b) of the Supplementary information. The calculated K_b values, along with the corresponding free energy of binding (ΔG_b) , are provided in Table 1.

The interaction of OFL-CTAB and OFL-SDS in aqueous solution reveals a clear preference for SDS over CTAB in terms of binding and micellar partitioning. Under typical aqueous conditions (Scheme 2), OFL exists with a localized positive charge on nitrogen (N⁺) in the piperazine ring and delocalized negative charge on a deprotonated carboxyl group (COO⁻). The N⁺ site facilitates strong electrostatic attraction with the anionic sulfate headgroup of SDS, enhancing micellar incorporation, further supported

by hydrophobic interactions with the surfactant tail. In contrast, CTAB's cationic headgroup shows weaker binding, likely due to electrostatic repulsion with N⁺ and diminished COO⁻ ionization at the working pH, resulting in reduced affinity and partitioning compared to SDS. These results not only confirm the favorable OFL-SDS interactions but also align with our previous findings on fluoroquinolone drugs such as gatifloxacin (Sohail et al. 2020), sparfloxacin (Sohail et al. 2021), moxifloxacin (Sohail et al. 2023), and gemifloxacin (Sohail et al. 2024) which similarly showed greater affinity for SDS compared to cationic surfactants such as CTAB and DTAB.

Cyclic Voltammetric studies

The cyclic voltammograms of OFL-CTAB and OFL-SDS systems are given in Fig. 8. It is clear from the voltammogram that the current value increases with increasing CTAB but decreases with SDS concentration, in the respective systems.

This noticeable trend in respective current values of anionic and cationic surfactants can be attributed to the establishment of an active electrochemical system for both OFL-CTAB/SDS complexes. Further, Langmuir relation (Eq. 12) was used for calculating the binding coefficient of OFL with CTAB and SDS (Mahajan et al. 2012).

$$\frac{1}{\Delta I_p} = \frac{1}{\Delta I_{p(max)}} + \frac{1}{\Delta I_{p(max)} K_b C}$$
 (12)

The binding parameters are defined as follows: K_b (binding constant), ΔI_p (current drop), and $\Delta I_{p(max)}$ (maximum current drop). Analysis of the $I/\Delta I_p$ versus I/C plots (Supplementary Information Fig. S3 a, b) gave K_b values for both OFL-CTAB and OFL-SDS systems (Table 4). The significantly lower Kb observed for the OFL-CTAB system

Scheme 2 Canonical forms of OFL in water



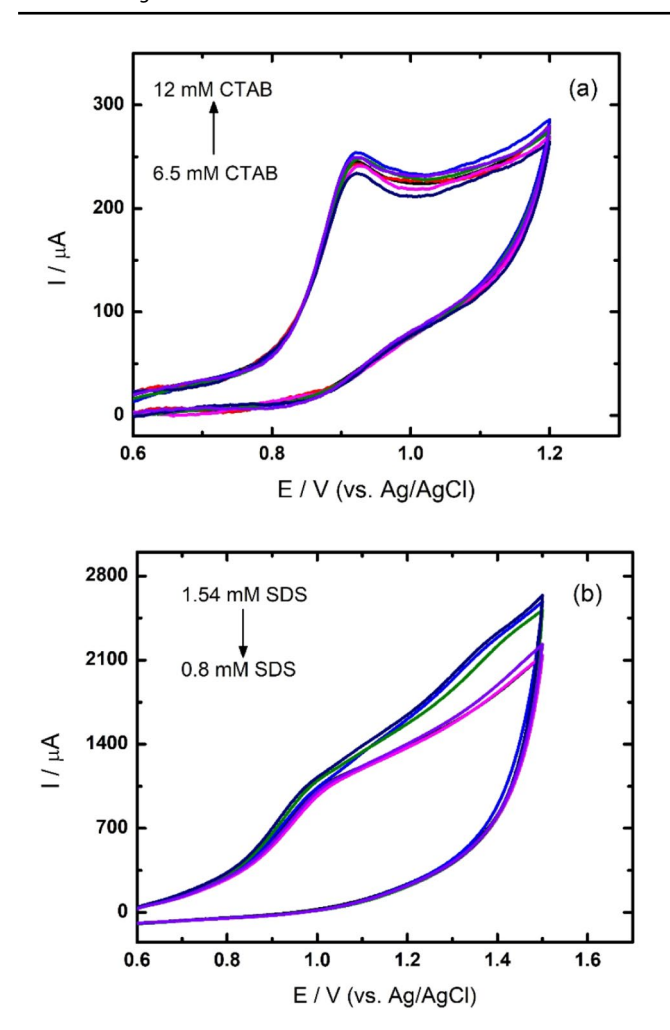


Fig. 8 Cyclic voltammograms of a 1 mM OFL-CTAB b 1 mM OFL-SDS (at 298.15 K)

compared to OFL-SDS reflects their distinct interaction mechanisms: while OFL-SDS binding is dominated by strong electrostatic interactions, the OFL-CTAB association primarily involves weaker hydrophobic forces.

The change in free energy (ΔG_b) for OFL-ionic surfactant interaction was calculated using following relation (Eq. (13)):

$$\Delta G_b = -RT \ln K_b \tag{13}$$

The negative Gibbs free energy values (ΔG_b) for both systems (Table 1) confirm the spontaneous nature of OFL binding with both anionic and cationic surfactants. Interestingly, the more negative ΔG_b observed for the OFL-SDS system compared to OFL-CTAB indicates a stronger binding affinity, consistent with the electrostatic-driven association between OFL and SDS. This thermodynamic conclusion is strongly supported by the excellent agreement between UV-Vis absorption and voltammetric measurements

(Table 1), which together provide compelling evidence for: (1) the spontaneous encapsulation of OFL within micellar structures, and (2) the distinct binding mechanisms operating in each surfactant system. The concordance between these complementary techniques reestablishes the reliability of our findings regarding drug-surfactant interactions.

Conclusion

This study provides a comprehensive analysis of the interactions between Ofloxacin (OFL) and the surfactants CTAB and SDS, explaining the complex interplay of forces that govern their behavior in micellar environments. By examining these interactions under varying temperature and surfactant concentration conditions, we uncovered significant ion-ion interactions at lower surfactant levels, which evolved into a broader network of ion-hydrophobic, hydrophilic-hydrophobic, and hydrophobic-hydrophobic interactions as concentrations increased. These findings, resulting from apparent molar volume (ϕ_v) and compressibility (K_s and ϕ_k) measurements, highlight the dynamic role of micellar structures in stabilizing OFL within solution.

UV–Visible spectroscopy and cyclic voltammetry further confirmed these observations, with binding constant (K_b) values and free energy changes indicating stronger OFL–SDS interactions compared to OFL–CTAB. The anionic SDS micelles demonstrated superior solubilization and encapsulation of OFL, driven by enhanced ion–ion interactions and favourable partitioning, as shown by differential absorbance and electrochemical data.

Ultimately, this research illuminates the critical role of surfactant charge and micellar architecture in modulating drug-surfactant interactions. These insights pave the way for designing micelle-based drug delivery systems that enhance solubility and facilitate targeted transport across biological membranes. By deepening our understanding of these molecular interactions, this work contributes meaningfully to the development of innovative pharmaceutical formulations.

Supplementary Information The online version contains supplementary material available at https://doi.org/10.1007/s00232-025-00357-0.

Acknowledgements The authors would like to acknowledge the Department of Chemistry at Forman Christian College (A Chartered University), Lahore, Pakistan, for their laboratory facilities, and logistical assistance.

Author Contributions SR was responsible for data collection, methodology development, original draft writing, validation, and formal analysis. AM contributed to formal analysis and investigation. MS provided supervision, project administration, writing (review and editing), and contributed to the methodology. AYK was involved in investigation, project administration, and funding acquisition.



Funding The authors gratefully acknowledge the financial support provided by the Higher Education Commission (HEC) of Pakistan under the HEC-NRPU Project No. 5476, which enabled the successful execution of this research work.

Data availability Data is provided within the manuscript or supplementary information files.

Declarations

Conflict of interest The authors declare no competing interests.

References

- Ahmed B, Anjum K, Alfakeer M et al (2024a) Interaction of sodium dodecyl sulfate and triton X-100 with ofloxacin drug using conductivity and UV-visible spectroscopic techniques in aqueous alcohols media at several temperatures. Colloids Surf A Physicochem Eng Asp 688:100. https://doi.org/10.1016/j.colsurfa.2024. 133608
- Ahmed B, Masood J, Shamim K et al (2024b) Impacts of different hydrotropes on the aggregation behavior and physicochemical parameters of sodium dodecyl sulfate and ofloxacin drug mixture at several temperatures. Colloid Polym Sci 302:1939–1956. https://doi.org/10.1007/s00396-024-05317-z
- Alalwani AK, Ahad S, Dhaher NHS (2023) Biomimetic cell membrane vehicles: navigating the blood–brain barrier for enhanced CNS drug delivery. Trends Pharm Biotechnol 1:48–63. https://doi.org/ 10.57238/tpb.2023.144292.1004
- Asghar Jamal M, Naseem B, Naz S et al (2020) Thermo-acoustic properties of maltose in aqueous amino acids system. J Mol Liq 309:112932. https://doi.org/10.1016/j.molliq.2020.112932
- Benesi HA, Hildebrand JH (1949) A spectrophotometric investigation of the interaction of iodine with aromatic hydrocarbons. J Am Chem Soc 71:2703–2707. https://doi.org/10.1021/ja01176a030
- Bhardwaj V, Bhardwaj T, Sharma K et al (2014) Drug-surfactant interaction: thermo-acoustic investigation of sodium dodecyl sulfate and antimicrobial drug (levofloxacin) for potential pharmaceutical application. RSC Adv 4:24935–24943. https://doi.org/10.1039/c4ra02177k
- Castillo-Sánchez JC, Cruz A, Pérez-Gil J (2021) Structural hallmarks of lung surfactant: lipid-protein interactions, membrane structure and future challenges. Arch Biochem Biophys. https://doi.org/10.1016/j.abb.2021.108850
- Chauhan S, Chauhan MS, Chauhan GS et al (2012a) Sound speed and density studies of interactions between cationic surfactants and aqueous gelatin solution. Int J Thermophys 33:279–288. https://doi.org/10.1007/s10765-011-1146-0
- Chauhan S, Sharma K, Rana DS et al (2012b) Conductance, apparent molar volume and compressibility studies of cetyltrimethylammonium bromide in aqueous solution of leucine. J Mol Liq 175:103–110. https://doi.org/10.1016/j.molliq.2012.07.029
- Chen H, Panagiotopoulos AZ (2019) Molecular modeling of surfactant micellization using solvent-accessible surface area. Langmuir 35:2443–2450. https://doi.org/10.1021/acs.langmuir.8b03440
- Christaki E, Marcou M, Tofarides A (2020) Antimicrobial resistance in bacteria: mechanisms, evolution, and persistence. J Mol Evol 88:26–40. https://doi.org/10.1007/s00239-019-09914-3
- Duval RE, Grare M, Demoré B (2019) Fight against antimicrobial resistance: we always need new antibacterials but for right bacteria. Molecules 24:1–9. https://doi.org/10.3390/molecules241731

- Eid HM, Elkomy MH, El Menshawe SF, Salem HF (2019) Development, optimization, and in vitro/in vivo characterization of enhanced lipid nanoparticles for ocular delivery of ofloxacin: the influence of pegylation and chitosan coating. AAPS Pharm-SciTech 20:1–14. https://doi.org/10.1208/s12249-019-1371-6
- Faizan M, Mukhtar F, Ashfaq M et al (2015) Physicochemical investigation of antibacterial Moxifloxacin interacting with quaternary ammonium disinfectants. Fluid Phase Equilib 406:47–54. https://doi.org/10.1016/j.fluid.2015.07.033
- Frank HS, Evans MW (1945) Free volume and entropy in condensed systems III. Entropy in binary liquid mixtures; Partial molal entropy in dilute solutions; Structure and thermodynamics in aqueous electrolytes. J Chem Phys 13:507–532. https://doi.org/10.1063/1.1723985
- Friedman HL, Krishnan CV (1973) Studies of hydrophobic bonding in aqueous alcohols: enthalpy measurements and model calculations. J Solution Chem 2:119–140. https://doi.org/10.1007/BF00651969
- Ghosh R, Hareendran H, Subramaniam P (2019) Adsorption of fluoroquinolone antibiotics at the gas—liquid interface using ionic surfactants. Langmuir 35:12839—12850. https://doi.org/10.1021/acs.langmuir.9b02431
- Gurney RW (1953) Ionic processes in solution. McGraw Hill, New York
- Kawamura H, Manabe M, Miyamoto Y et al (1989) Partition coefficients of homologous ω-phenylalkanols between water and sodium dodecyl sulfate micelles. J Phys Chem 93:5536–5540. https://doi.org/10.1021/j100351a042
- Kumar D, Rub MA (2018a) Studies of interaction between ninhydrin and Gly-Leu dipeptide: influence of cationic surfactants (m-s-m type Gemini). J Mol Liq 269:1–7. https://doi.org/10.1016/j.molliq.2018.08.002
- Kumar D, Rub MA (2018b) Interaction of ninhydrin with chromiumglycylglycine complex in the presence of dimeric gemini surfactants. J Mol Liq 250:329–334. https://doi.org/10.1016/j.molliq. 2017.11.172
- Liu D, Yang F, Xiong F, Gu N (2016) The smart drug delivery system and its clinical potential. Theranostics 6:1306–1323. https://doi.org/10.7150/thno.14858
- Lomesh SK, Nathan V, Bala M, Thakur P (2019) Volumetric and acoustic methods for investigating molecular interactions of antibiotic drug doxycycline hyclate in water and in aqueous solution of sodium chloride and potassium chloride at different temperatures (293.15–313.15) K. J Mol Liq 284:241–251. https://doi.org/ 10.1016/j.molliq.2019.04.006
- Mahajan S, Sharma R, Mahajan RK (2012) An investigation of drug binding ability of a surface active ionic liquid: micellization, electrochemical, and spectroscopic studies. Langmuir 28:17238– 17246. https://doi.org/10.1021/la303193n
- Nadeem I, Yasmeen F, Sohail M et al (2024) Chemopreventive catechin hydrate interaction with self-aggregated structures – a thermoacoustic, spectroscopic and electrochemical study. J Mol Liq. https://doi.org/10.1016/j.molliq.2024.124295
- Naseem B (2020) Effect of alkyl chain length of 1-alkanols on solution behavior of bactericidal antibiotic in terms of thermo-acoustic parameters. J Mol Liq 307:112991. https://doi.org/10.1016/j.molliq.2020.112991
- Naseem B, Iftikhar M (2017) Investigation on molecular interactions of antibiotics in alcohols using volumetric and acoustic studies at different temperatures. J Chem Thermodyn 104:239–251. https:// doi.org/10.1016/j.jct.2016.09.037
- Pathania D, Gupta D, Kothiyal NC et al (2016) Preparation of a novel chitosan-g-poly(acrylamide)/Zn nanocomposite hydrogel and its applications for controlled drug delivery of ofloxacin. Int J Biol Macromol 84:340–348. https://doi.org/10.1016/j.ijbiomac.2015. 12.041



- Rabbani S, Abid H, Khan AY et al (2025) Volumetric, acoustic, and conductometric studies of ionic surfactants in aqueous ammonium acetate-ethylene glycol deep eutectic solvent. J Mol Liq 433:127971. https://doi.org/10.1016/j.molliq.2025.127971
- Santosh MS, Bhat DK, Bhat AS (2009) Molecular interactions in glycylglycine-mncl2 aqueous solutions at (288.15, 293.15, 298.15, 303.15, 308.15, 313.15, and 318.15) k. J Chem Eng Data 54:2813–2818. https://doi.org/10.1021/je800732f
- Sharma K, Chauhan S (2014) Apparent molar volume, compressibility and viscometric studies of sodium dodecyl benzene sulfonate (SDBS) and dodecyltrimethylammonium bromide (DTAB) in aqueous amino acid solutions: a thermo-acoustic approach. Thermochim Acta 578:15–27. https://doi.org/10.1016/j.tca.2013.12.
- Sohail M, Rahman HMAU, Asghar MN (2020) Gatifloxacin-ionic surfactant interactions: volumetric, acoustic, voltammetric, and spectroscopic studies. J Surfactants Deterg. https://doi.org/10. 1002/jsde.12480
- Sohail M, Rahman HMAU, Asghar MN (2021) Thermo-acoustic, spectroscopic, and electrochemical investigation of sparfloxacin–ionic surfactant interactions. J Mol Liq 340:117186. https://doi.org/10.1016/j.molliq.2021.117186
- Sohail M, Rahman HMAU, Asghar MN (2023) Drug—ionic surfactant interactions: density, sound speed, spectroscopic, and electrochemical studies. Eur Biophys J 52:735–747. https://doi.org/10.1007/s00249-023-01689-2

- Sohail M, Rahman HMA, ur Nadeem Asghar M, Shoukat S (2024) Apparent molar volume, compressibility, and spectroscopic studies of ionic surfactants in aqueous solutions of antibiotic gemi-floxacin. J Dispers Sci Technol 45:1931–1941. https://doi.org/10.1080/01932691.2023.2239329
- Suresh A, Gonde S, Mondal PK et al (2020) Improving solubility and intrinsic dissolution rate of ofloxacin API through salt formation via mechanochemical synthesis with diphenic acid. J Mol Struct 1221:128806. https://doi.org/10.1016/j.molstruc.2020.128806
- Yan Z, Liu R, Wu S et al (2013) Effect of temperature on the interactions of glycyl dipeptides with sodium perfluorooctanoate in aqueous solution: volumetric, conductometric, and spectroscopic study. J Chem Thermodyn 57:360–366. https://doi.org/10.1016/j. jct.2012.09.018

Publisher's Note Springer Nature remains neutral with regard to jurisdictional claims in published maps and institutional affiliations.

Springer Nature or its licensor (e.g. a society or other partner) holds exclusive rights to this article under a publishing agreement with the author(s) or other rightsholder(s); author self-archiving of the accepted manuscript version of this article is solely governed by the terms of such publishing agreement and applicable law.

Authors and Affiliations

Saqib Rabbani¹ · Areesha Maryam¹ · Muhammad Sohail² · Athar Yaseen Khan¹

- Muhammad Sohail
 muhammadsohail@westlake.edu.cn
- Athar Yaseen Khan
 atharkhan@fccollege.edu.pk
 Saqib Rabbani
 saqib.rrabbani@gmail.com
 Areesha Maryam
 areeshamaryam32@gmail.com

- Department of Chemistry, Forman Christian College (A Chartered University), Zahoor Elahi Rd, Gulberg III, Lahore 54600, Pakistan
- School of Engineering, Westlake University, Hangzhou, China

